

# Capillary nematization of hard colloidal platelets confined between two parallel hard walls

Hendrik Reich<sup>1</sup> and Matthias Schmidt<sup>1,2</sup>

<sup>1</sup> Institut für Theoretische Physik II, Heinrich-Heine-Universität Düsseldorf, Universitätsstraße 1, D-40225 Düsseldorf, Germany

<sup>2</sup> H H Wills Physics Laboratory, University of Bristol, Royal Fort, Tyndall Avenue, Bristol BS8 1TL, UK

Received 28 April 2007, in final form 30 April 2007

Published 19 July 2007

Online at [stacks.iop.org/JPhysCM/19/326103](http://stacks.iop.org/JPhysCM/19/326103)

## Abstract

We use density functional theory to study the capillary phase behaviour of a discotic system of colloidal platelets that are confined in a planar slit pore. The model plates have circular shape, continuous orientations and vanishing thickness; they interact via hard-core repulsion with each other and with the walls which induces homeotropic wall anchoring of the nematic director. We find that the isotropic–nematic capillary binodal is shifted to lower values of the chemical potential as compared to bulk isotropic–nematic coexistence. Capillary isotropic–nematic coexistence vanishes below a critical wall separation distance which is significantly larger than it is in a reference system of thin hard (Onsager) rods confined between two parallel hard walls that act on the particle centres.

## 1. Introduction

The bulk phase behaviour of dispersions of nonspherical colloidal particles can be considerably more complex than that of dispersions of spheres due to the occurrence of partially ordered, liquid crystalline phases in such systems. The stability of liquid crystals (LCs) originates from complex particle shapes and is accompanied with properties between those of liquids and those of solids. A simple example of a LC phase transformation is that between an isotropic (I) fluid and an orientationally ordered nematic (N) fluid. The nematic phase is characterized by macroscopic orientational order; the particles align preferentially along a common direction, called the nematic director. The symmetry breaking in director space and the resulting elastic behaviour of the nematic phase resemble a crystal, while the spatial distribution of position coordinates remains homogeneous like in a liquid. The isotropic–nematic (IN) transition was first observed experimentally in suspensions of (rod-like) tobacco mosaic virus particles [1, 2], and a famous theoretical description was given by Onsager [3]. Cast into modern language, this theory can be viewed as a truncation of the Taylor expansion of the Helmholtz excess free

energy functional at second order in density and becomes exact, due to a scaling argument, in the limit of thin rods [4]. However, such scaling does not hold for (vanishingly) thin hard platelets; when applied to this system the Onsager theory is known to predict the bulk IN transition correctly to be of first order, but to overestimate the transition densities and value of the nematic order parameter at coexistence quite severely as compared to simulation results [5, 6]. The peculiar features of the bulk IN transition of hard platelets are the very small density jump at coexistence and the very low value of the nematic order parameter,  $S \sim 0.5$ , in the coexisting nematic phase.

During recent years considerable experimental, simulation and theoretical work has been devoted to gaining understanding of the behaviour of platelet dispersions. A well-established experimental model system is gibbsite platelets dispersed in toluene, for which the existence of the IN transition was observed with polarization microscopy [7]. In the same system the nematic–columnar phase transition [8], the hexagonal-columnar liquid crystal phase [9], and gelation and nematic ordering [10] were investigated. Also the influence of external potentials was considered, e.g. that of gravity [11, 12] and of electric [13] and magnetic fields [14]. Platelike clay particles [15, 16] and mixtures of colloidal platelets and polymers [17, 18] have also received attention. Theoretical investigations were devoted to the influence of gravity on phase behaviour [19], and the phenomenon of nematic density inversion [20]. An interaction site model for lamellar colloids was investigated [21]. The phase diagram of a mixture of hard colloidal spheres and discs was obtained from a free volume approach [22], and the free IN interface in fluids of charged platelike colloids was investigated using the Zwanzig model with discrete orientations [23]. Reference [24] is devoted to the effects caused by polydispersity in a mixture of rods and platelets. A model fluid of hard platelike particles has also been used to describe the structure factor of macromolecular solutions of stilbenoid dendrimers [25].

The presence of a substrate commonly leads to rich phenomenology of surface phase transitions. The smooth hard planar wall is a basic model for a substrate which despite its simplicity induces intriguing effects. For hard-core models energy is irrelevant and one refers to ‘entropic wetting’ [26]; examples include ordering of rods near a hard wall [27], the uniaxial–biaxial transition of hard rods [28–30], and prefreezing of hard spheres [31]. Also the entropic torque acting on a single hard rod in a solvent of hard spheres close to the wall was investigated [32]. The isotropic phase of platelets in contact with a wall has been considered in [33] using Onsager theory, and results were compared to those for a hard-rod fluid. For the Zwanzig model of platelets with restricted orientations [34] wetting and capillary effects were investigated [35], as well as bulk and interfacial properties of binary mixtures [36].

We have recently developed a density functional theory (DFT) for platelets [37] based on fundamental measure theory (FMT), an approach that was originally developed for additive hard-sphere mixtures by Rosenfeld [38]. The platelets are modelled as having circular shape and vanishing thickness; they possess continuous orientations, which is somewhat more realistic than in the Zwanzig model where orientations are restricted to the three Cartesian directions. The FMT of [37] was shown to give very accurate results for bulk and interfacial properties of model platelet dispersions as compared to results from large-scale Monte Carlo computer simulations [39, 40]. It was also shown that the FMT improves significantly over results obtained from the Onsager theory. A peculiar feature of the model is that the value of the IN interfacial tension is unusually low. From measuring the capillary rise of the nematic phase at a vertical substrate a corresponding experimental value for the IN interface tension was obtained [39], in reasonable agreement with the theoretical prediction. It was also demonstrated that a hard wall is wetted completely by the nematic phase upon approaching IN coexistence from the (low-density) isotropic side [39, 40].

In this paper we use the theory of [37] to investigate the capillary effects that arise when the hard-platelet system is confined in a planar slit pore. It is well known that situations of strong confinement can have a profound effect on the phase behaviour and structure of condensed matter. A prominent effect that occurs in simple liquids is capillary condensation, i.e. the pore stabilizes the liquid phase at statepoints where the gas is stable in bulk [41, 42]. The analogue in the case of the IN transition is capillary nematization where the presence of the capillary stabilizes the nematic at statepoints where the bulk is isotropic. A corresponding shift of the IN transition to lower chemical potentials occurs. Confinement has been considered for different types of molecular liquid crystals and of colloidal dispersions, see e.g. [43, 44] for the behaviour of confined thermotropic liquid crystals. Reference [45] investigates hard rods confined by two parallel hard walls using integral equations and computer simulations. The authors examine the dependence of the free energy on the separation of the walls and conclude that capillary nematization should occur. References [28, 29] examine capillary nematization for biaxial hard rods within the Zwanzig model, and [30] confirms these results with Monte Carlo simulations. Reference [46] investigates a confined soft ellipsoid fluid with DFT, and in [47] computer simulations of long thin hard rods in a quasi-two-dimensional planar geometry were performed. In [48, 49], a detailed investigation of hard rods in a capillary with walls acting on the centres of the rods and an additional external potential is carried out. The authors find capillary nematization as well as capillary smectization, i.e. a shift of the nematic–smectic phase transition to lower chemical potentials upon confining the system. Much less work has been devoted to systems of confined hard-platelet fluids. In [35] the authors investigate the wetting and capillary nematization behaviour of binary hard-platelet (and also hard-rod) fluids using the Zwanzig model. They obtain density profiles and find a capillary critical point upon decreasing the wall separation. We comment on the very recent computer simulation study published in [50] at the end of this paper. Here we investigate the same phenomenon using a hard-platelet fluid with continuous orientations. As a well-studied reference system, we use a confined system of thin hard rods that we study with Onsager theory.

This paper is organized as follows. In section 2 we describe the model interactions and give an overview of DFT. We present results for capillary phenomena of plates and rods in section 3 and conclude in section 4.

## 2. The model and density functional theory

We consider a fluid of infinitely thin hard circular platelets of diameter  $D$ . The platelets interact with a hard-core pair potential  $\phi(\mathbf{r}, \boldsymbol{\omega}, \boldsymbol{\omega}')$  that depends on the centre-to-centre distance  $\mathbf{r}$  between both platelets and on their orientations,  $\boldsymbol{\omega}$  and  $\boldsymbol{\omega}'$ , taken to be unit vectors perpendicular to the plane of the respective particle.  $\phi(\mathbf{r}, \boldsymbol{\omega}, \boldsymbol{\omega}')$  is infinite provided that the two particles overlap and vanishes otherwise. The system is confined by a pair of planar smooth hard walls, which we take to be perpendicular to the  $z$ -direction and to be located at  $z = 0$  and  $H$ , such that only the slab  $0 \leq z \leq H$  is accessible to the particles. Hence the interaction between the hard walls and a platelet is described by an external potential,

$$V_{\text{ext}}(z, \theta) = \begin{cases} 0 & (D/2) \sin \theta \leq z \leq H - (D/2) \sin \theta \\ \infty & \text{otherwise} \end{cases}, \quad (1)$$

where  $\theta$  is the angle between the  $z$ -direction and the particle orientation  $\boldsymbol{\omega}$ , which we can choose to be in the range  $0 \leq \theta \leq \pi/2$  due to the inflection symmetry,  $\boldsymbol{\omega} \rightarrow -\boldsymbol{\omega}$ , of the particles. See figure 1 for an illustration of the model.

The one-body density distribution of the particles is denoted by  $\rho(\mathbf{r}, \boldsymbol{\omega})$ , where  $\mathbf{r}$  is the position coordinate of the particle centre. The bulk density is denoted by  $\rho$  and the

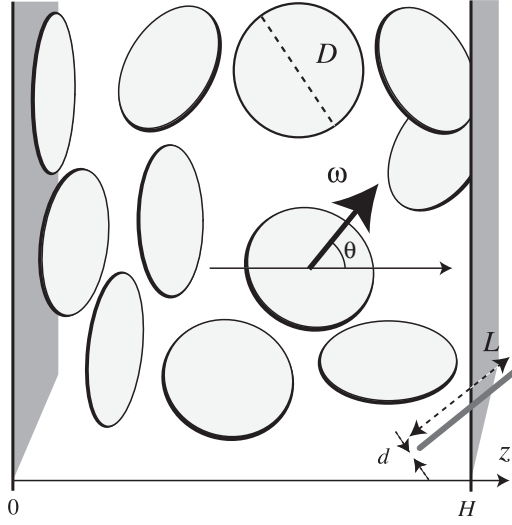


**Figure 1.** Model of hard platelets of diameter  $D$  and vanishing thickness confined between two planar parallel hard walls with separation distance  $H$ . The angle between the  $z$ -direction, perpendicular to the walls, and the platelet orientation  $\omega$  is denoted by  $\theta$ . In a reference system of thin hard rods of length  $L$  and thickness  $d \ll L$  the hard walls act on the centres of the particles.

normalization is chosen such that  $\rho = \int d\mathbf{r} d\omega \rho(\mathbf{r}, \omega) / (4\pi V)$ , where  $V$  is the system volume. As we do not expect biaxiality to occur, we can assume invariance with respect to rotations around the  $z$ -axis, as well as translational invariance in the  $x$ - and  $y$ -directions. The remaining relevant angle  $\theta$  is that between the orientation  $\omega$  and the  $z$ -axis; see figure 1. It follows that the (number) density distribution  $\rho(\mathbf{r}, \omega) = \rho(z, \theta)$ .

As a reference system we use the well-studied model of thin hard rods of length  $L$  and diameter  $d$  in the Onsager limit where  $d/L \rightarrow 0$ . A planar capillary that induces homeotropic alignment is constituted by two parallel hard walls that act on the particle *centres* such that

$$V_{\text{ext}}(z) = \begin{cases} 0 & 0 \leq z \leq H \\ \infty & \text{otherwise.} \end{cases} \quad (2)$$

Again planar geometry is assumed, where the only relevant spatial coordinate is  $z$  and the remaining angle  $\theta$  is that between the orientation  $\omega$  (along the rod) and the  $z$ -axis, as sketched in figure 1.

In DFT the grand potential is expressed as a functional of the one-body density distribution [51],

$$\tilde{\Omega}([\rho], \mu) = F_{\text{id}}[\rho] + F_{\text{exc}}[\rho] + \int d\mathbf{r} \int \frac{d\omega}{4\pi} \rho(\mathbf{r}, \omega) (V_{\text{ext}}(\mathbf{r}, \omega) - \mu), \quad (3)$$

where  $F_{\text{exc}}[\rho]$  is the excess (over ideal gas) contribution to the total (Helmholtz) free energy functional that arises from interparticle interactions,  $V_{\text{ext}}(\mathbf{r}, \omega)$  is an external potential acting on the particles,  $\mu$  is the chemical potential, and the ideal gas (Helmholtz) free energy functional for uniaxial rotators is given by

$$F_{\text{id}}[\rho] = k_{\text{B}}T \int d\mathbf{r} \int \frac{d\omega}{4\pi} \rho(\mathbf{r}, \omega) (\ln(\rho(\mathbf{r}, \omega)\Lambda^3) - 1), \quad (4)$$

where  $k_{\text{B}}$  is Boltzmann's constant,  $T$  is the absolute temperature, and  $\Lambda$  is the (irrelevant) thermal wavelength for which we choose  $\Lambda = D/2$ ; the dependence on volume  $V$  and

temperature has been suppressed in the notation. In the following we use the scaled chemical potential  $\mu^* = \beta\mu$  with  $\beta = 1/k_B T$ . For any given external potential  $V_{\text{ext}}(\mathbf{r}, \boldsymbol{\omega})$ , minimizing the grand potential with respect to the one-body density distribution  $\rho(\mathbf{r}, \boldsymbol{\omega})$  gives the equilibrium density profile,

$$\frac{\delta\tilde{\Omega}[\rho]}{\delta\rho(\mathbf{r}, \boldsymbol{\omega})} = 0, \quad (5)$$

which can be rewritten, using equation (3), as an Euler–Lagrange equation

$$k_B T \ln(\rho(\mathbf{r}, \boldsymbol{\omega})\Lambda^3) - k_B T c_1([\rho], \mathbf{r}, \boldsymbol{\omega}) + V_{\text{ext}}(\mathbf{r}, \boldsymbol{\omega}) = \mu, \quad (6)$$

where  $c_1([\rho], \mathbf{r}, \boldsymbol{\omega}) = -(k_B T)^{-1} \delta F_{\text{exc}}[\rho] / \delta\rho(\mathbf{r}, \boldsymbol{\omega})$  is the one-body direct correlation functional. One systematic way to write down the excess free energy functional is to expand it in a virial series,

$$F_{\text{exc}}[\rho] = -\frac{k_B T}{2} \int d\mathbf{r} \int \frac{d\boldsymbol{\omega}}{4\pi} \int d\mathbf{r}' \int \frac{d\boldsymbol{\omega}'}{4\pi} \rho(\mathbf{r}, \boldsymbol{\omega}) \rho(\mathbf{r}', \boldsymbol{\omega}') f(\mathbf{r} - \mathbf{r}', \boldsymbol{\omega}, \boldsymbol{\omega}') + O(\rho^3), \quad (7)$$

where  $f(\mathbf{r}, \boldsymbol{\omega}, \boldsymbol{\omega}') = \exp(-\beta\phi(\mathbf{r}, \boldsymbol{\omega}, \boldsymbol{\omega}')) - 1$  is the Mayer function that for hard bodies is  $-1$  if the two particles overlap and vanishes otherwise. In practice, one has to resort to approximations to  $F_{\text{exc}}[\rho]$  and Onsager's theory relies on truncating equation (7) at second order in density. For platelets we use the theory of [37] that possesses the exact second-order contribution, but also contains an (approximative) contribution of third order in density; for details see [37, 39]. In the reference case of rods, we use the Onsager theory.

In order to facilitate a quantitative comparison between results for the two models, we scale the density distributions with the second virial coefficient of the respective pair potential, i.e. for platelets  $B_2 = \pi^2 D^3 / 16 = 0.61685 D^3$ , and for rods  $B_2 = \pi L^2 d / 4 = 0.785398 L^2 d$ . We hence define the respective scaled densities  $c(z, \theta) = B_2 \rho(z, \theta)$  as

$$c(z, \theta) = \frac{\pi}{4} d L^2 \rho(z, \theta) \quad (\text{rods}), \quad c(z, \theta) = \frac{\pi^2}{16} D^3 \rho(z, \theta) \quad (\text{plates}). \quad (8)$$

The inhomogeneous density distributions in the capillary are conveniently analysed using an orientation-averaged density profile,

$$c(z) = \int_0^{\pi/2} d\theta \sin(\theta) c(z, \theta), \quad (9)$$

and a nematic order parameter profile, defined as

$$S(z) = \frac{1}{c(z)} \int_0^{\pi/2} d\theta \sin(\theta) c(z, \theta) P_2(\cos \theta), \quad (10)$$

where  $P_2(x) = (3x^2 - 1)/2$  is the second Legendre polynomial. The corresponding spatially averaged quantities are obtained as

$$\langle c \rangle = \frac{1}{H} \int_0^H dz c(z), \quad (11)$$

and

$$\langle S \rangle = \frac{1}{H} \int_0^H dz S(z). \quad (12)$$

Capillary coexistence is found through the condition that at a given value of the plate separation distance  $H$  and of the chemical potential  $\mu$  both phases possess the same value of the grand potential  $\Omega$  per unit area (equality of the temperatures in both phases is trivial for hard-core systems).

Our numerical implementation to solve equation (6) uses an equidistant grid in the  $z$ -direction with 40 grid points per diameter  $D$  in the case of plates and 100 grid points per length  $L$  in the case of rods. The angle  $\theta$  is discretized on a non-equidistant grid with 20 (100) grid points in the interval  $[0; \pi/2]$  for plates (rods). As a minimization procedure we use molecular dynamics-type simulated annealing [52–54]. For some more details about the numerics that also apply to the current study see [40].

### 3. Results

The variation of the phase coexistence densities for confined hard platelets as a function of the scaled inverse wall separation distance  $D/H$  is shown in figure 2(a). As found previously [37], the values in bulk,  $D/H \rightarrow 0$ , as obtained from the DFT agree well with results from simulations [5, 6]. For increasing values of  $D/H$  (and thus confining the system more strongly) we find an initial increase in both coexistence densities. Indeed the low-density coexistence phase for finite values of  $D/H$  possesses a certain degree of nematic order (discussed in detail below) which is induced by the orientational ordering effect of the walls. One could rightfully refer to this as a paranematic phase, but we will use in the following the term isotropic phase, as is commonly done for such confined states.

The increase of the average density is due to the presence of adsorption layers at both walls which contribute significantly to  $\langle c \rangle$ , even for small values of  $D/H$ . With further decreasing the wall separation distance (and hence increasing  $D/H$ ) the isotropic coexistence density continues to increase, but does this more slowly. We attribute this to the shift of the IN transition to lower chemical potentials, which is an effect in the opposite direction to the density increase due to the adsorption layer. The nematic coexistence density, on the other hand, is maximal at around  $D/H = 0.08$  (or  $H = 12.5D$ ) and decreases for smaller plate separation distances (larger values of  $D/H$ ). Ultimately the binodal terminates at an upper critical point,  $D/H = 0.172$  (or  $H = 5.8D$ ). Close to the capillary critical point the numerical effort is very demanding, which gives rise to some small numerical artefacts that are apparent in figure 2. The chemical potential at coexistence,  $\mu_{\text{coex}}^*$ , shifts to smaller values upon confining the system (increasing  $D/H$ ); see the inset of figure 2(a). This demonstrates that capillary nematization does indeed occur, i.e. that (over a range of statepoints) the capillary is in a nematic state in equilibrium with an isotropic bulk.

We next compare our density functional results for the capillary binodal with the prediction obtained from the Kelvin equation [41, 42]; see applications of the Kelvin equation for simple fluids in slit pores in [41, 42] and for a lattice model of the IN transition in [55]. The Kelvin equation for the present case reads

$$\Delta\mu = \frac{2\gamma_{\text{IN}}}{H(\rho_{\text{N}} - \rho_{\text{I}})}, \quad (13)$$

where  $\Delta\mu$  is the change of the chemical potential at capillary coexistence with respect to the bulk coexistence values and  $\gamma_{\text{IN}}$  is the interfacial tension of the free IN interfaces, as is appropriate in the present situation where the nematic phase wets a (single) hard wall completely [39, 40]. With the value  $\gamma_{\text{IN}}D^2/k_{\text{B}}T = 0.026624$  of [39] and  $\rho_{\text{N}}D^3 - \rho_{\text{I}}D^3 = 0.4$  we obtain  $\Delta\mu$  as a function of  $H$ ; the result is shown in the inset of figure 2(a). The predictions of the Kelvin equation for the capillary coexistence chemical potential are in good agreement with the results from the calculations for  $D/H = 0.086$  (which corresponds to a capillary width of  $H = 11.6D$ ) but become increasingly poor for larger values of  $D/H$ . Such behaviour could be expected as the Kelvin equation is valid only for  $H \gg D$ .

In the following we compare the above finding to the capillary phase behaviour of rods. Confinement of rods by walls that act on the particle centres and hence induce homeotropic

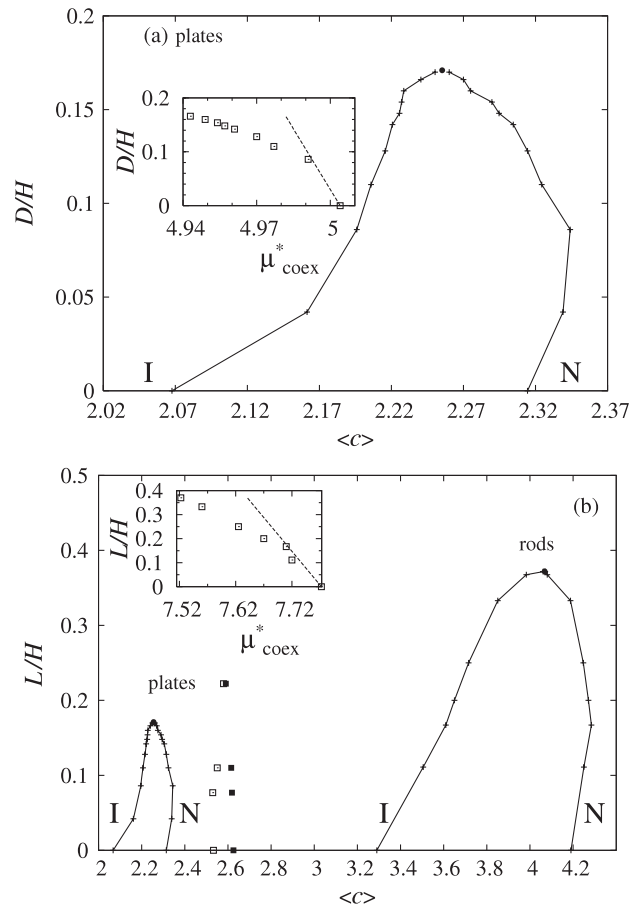


**Figure 2.** (a) Variation of the average isotropic and nematic coexistence density  $\langle c \rangle$  (horizontal axis) with the scaled inverse capillary width  $D/H$  (vertical axis) for hard platelets between parallel hard walls. The average density  $\langle c \rangle$  is defined via equations (8) and (11); the symbols represent results from FMT calculations, the lines are a guide to the eye. The capillary critical point (full circle) is located at  $\langle \rho \rangle = 2.26$  and  $D/H = 0.172$  ( $H = 5.8D$ ). The inset shows the variation of the (scaled) chemical potential at coexistence,  $\mu_{\text{coex}}^*$  (horizontal axis), with the inverse scaled plate separation distance  $D/H$  (vertical axes), as obtained from the full DFT calculation (symbols) and from the Kelvin equation (line). (b) Same as (a), but as obtained from Onsager theory for hard rods confined between hard walls that act on the particle centres. The critical point (full circle) is located at  $\langle c \rangle = 4.07$  and  $L/H = 0.373$  ( $H = 2.68L$ ). For comparison the result for platelets from part (a) is replotted (dashed line). Also shown are the results from Gibbs ensemble computer simulations [50] for the isotropic (open squares) and nematic (filled squares) coexistence densities for a system of hard cut spheres with aspect ratio 0.1.

anchoring has been considered in detail before [48, 49]. We have used the Onsager functional to reconsider this situations as a reference case. Figure 2(b) shows the variation of the average density  $\langle c \rangle$  at coexistence with the scaled inverse plate separation distance  $L/H$ . Both the isotropic and nematic coexistence densities increase with increasing values of  $L/H$ . While this increase holds for the isotropic density up to the critical point, the nematic density starts to decrease beyond a maximum at  $L/H = 0.16$ . The binodal ends it a critical point with  $L/H = 0.372$ . Again we apply the Kelvin equation (13) to calculate the shift of the chemical potential. The results are plotted in the inset of figure 2(b). Good agreement is found with the

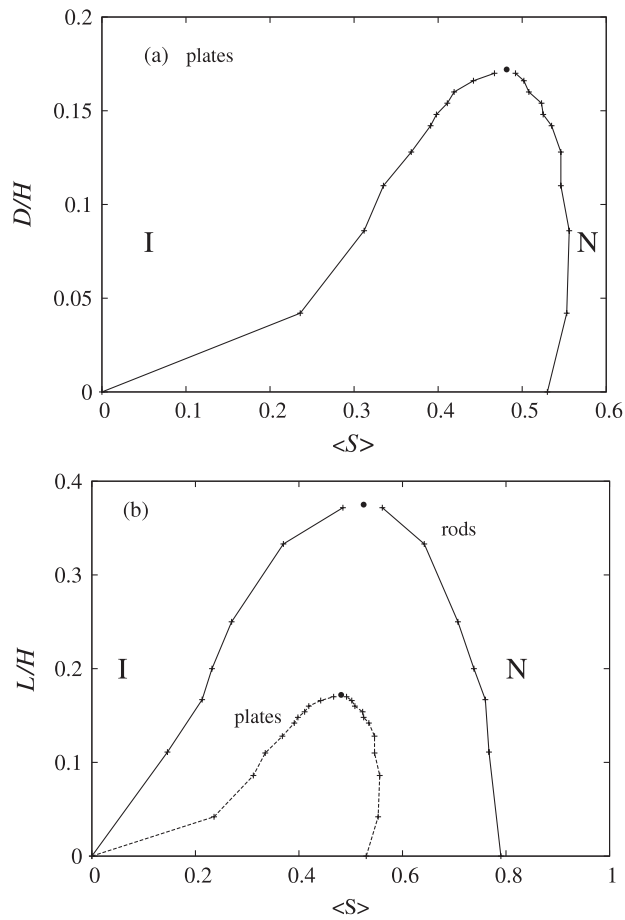


**Figure 3.** (a) Variation of the average order parameter  $\langle S \rangle$  (horizontal axis), defined via equation (12), for the isotropic and nematic phase at capillary coexistence as a function of the inverse capillary width  $D/H$  (vertical axis) as obtained from FMT for hard platelets between parallel hard walls. (b) Same as (a), but as obtained from Onsager theory for hard rods confined between parallel hard walls that act on the midpoints of the particles; here the inverse capillary width is  $L/H$ . For comparison the result for plates from (a) is also shown (dashed line).

data obtained from the full numerical DFT for small values of  $L/H$ ; for  $L/H$  closer to the critical point the predictions become increasingly poor.

The variation of the average nematic order  $\langle S \rangle$  along the capillary coexistence binodal confirms the scenario; see figure 3(a) for the results for platelets. The value at the isotropic coexistence branch increases with increasing  $D/H$ , up to the critical value. The nematic coexistence branch possesses a maximum at about  $D/H = 0.08$  (or  $H = 12.5D$ ). The behaviour of the order parameter  $\langle S \rangle$  for rods differs slightly from that for platelets; see figure 3(b). The value at isotropic coexistence decreases monotonically upon confining the system, but the nematic coexistence curve exhibits no maximum.

In figure 4(a) we plot density profiles  $c(z)$  for isotropic and nematic states at coexistence for typical values of the capillary width of the confined platelet system,  $H/D = 6, 6.5, 9.05, 11.55$ . The density in the centre of the capillary,  $z = H/2$ , increases from  $c(z = H/2) = 2.063$  to  $c(z = H/2) = 2.073$  upon reducing the plate separation distance

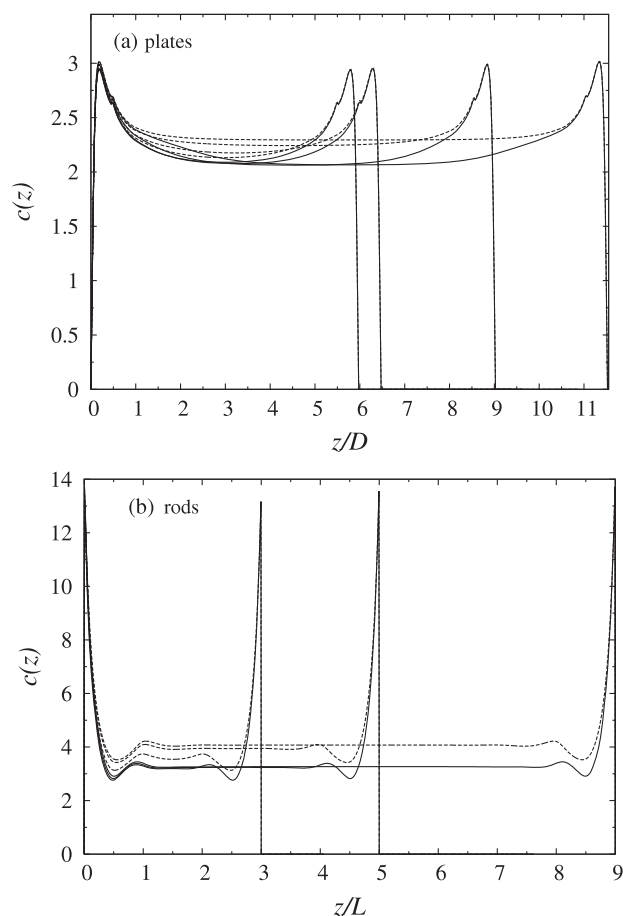


**Figure 4.** (a) Scaled density profiles  $c(z)$  as a function of the scaled distance from one of the walls,  $z/D$ , for  $H/D = 6, 6.5, 9.05, 11.55$  (from left to right) for hard platelets between parallel hard walls. Shown are the isotropic (full line) and nematic (dashed line) profiles at capillary coexistence. The coexistence chemical potential decreases from  $\mu^* = 4.991$  at  $H/D = 11.55$  to  $\mu^* = 4.943$  at  $H/D = 6$ . (b) Scaled density profile  $c(z)$  as a function of the distance from one of the walls,  $z/L$ , for  $H/L = 3, 5, 9$  (from left to right) for hard rods confined between parallel hard walls that act on the particle centres. Shown are isotropic (full line) and nematic (dashed line) coexistence profiles. The coexistence chemical potential decreases from  $\mu^* = 7.72$  at  $H/L = 9$  to  $\mu^* = 7.56$  at  $H/L = 3$ .

from  $H/D = 11.55$  to  $6.5$ , although the chemical potential at coexistence *decreases* in this case, as discussed above. This effect is related to the fact that for  $H/D = 6.5$  the wetting films of each wall ‘see’ each other and so shift the density to a higher value. Corresponding density profiles  $c(z)$  as a function of  $z$  for the confined rod system with capillary widths of  $H/L = 3, 5, 9$  are shown in figure 4(b). In the centre of the capillary,  $z = H/2$ , the values of the density at coexistence are almost reached for the cases  $H/L = 9$  and also  $5$ . The maximum of the density profile  $c(z)$  is directly at the wall.

The order parameter profiles  $S(z)$  in the coexisting isotropic and nematic states are plotted in figure 5(a) for the same values of  $H/D$  as the density profiles in figure 4(a). The variation of  $S(z)$  with  $z$  is similar to that at a single wall [40]. Here, however, capillary effects can be

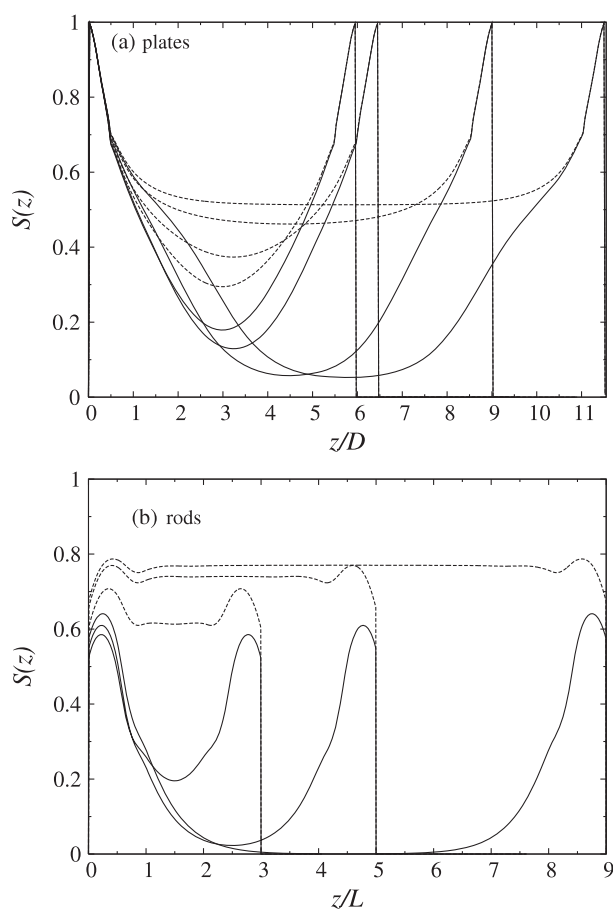


**Figure 5.** Order parameter profile  $S(z)$  as a function of the scaled distance  $z/D$  for hard platelets between parallel hard walls for the same statepoints at capillary coexistence as in figure 4(a). (b) Order parameter profile  $S(z)$  for hard rods between parallel hard walls that act on the particle centres as a function of  $z/L$  for the same statepoints as in figure 4(b).

clearly observed for  $H/D = 6.5$  and 6; see figure 5(a): the value of the order parameter for the isotropic coexistence profile in the middle of the capillary is  $S > 0.15$ , significantly larger than zero (as it is in the isotropic bulk). The nematic profile in the centre of the capillary is  $S(z = H/2) = 0.4$ , a value that is lower than that of the bulk nematic at coexistence; this is consistent with the shift of the chemical potential at capillary coexistence to lower values than in bulk at coexistence.

In contrast to the behaviour of the density profiles for the confined rod system—recall figure 4(b)—the maximum of the order parameter profile  $S(z)$  is surprisingly *not* located directly at the wall; see figure 5(b). This is in agreement with the profiles obtained in [48]. When looking at the profiles for  $H/L = 3$ , relatively close to the critical capillary width at  $H/L = 2.68$ , one finds that the capillary effects are more pronounced. In the centre of the capillary the value of the order parameter is significantly larger than zero. As observed for  $H/L = 5$  and 9, the maximum of the density is at the wall, while the maximum of the order parameter is shifted away from the wall.

## 4. Conclusions

In conclusion, we have investigated the behaviour of hard colloidal platelets of diameter  $D$  confined inside of a capillary that is constituted by two parallel planar hard walls. We find a critical plate separation distance of  $H = 5.8D$ ; for smaller values of  $H$  the capillary phase separation ceases to exist.

We have carried out reference calculations of a system of hard rods confined between parallel hard walls that act on the particle centres. This type of wall induces similar alignment to that of the hard (impenetrable) walls acting on the platelets. Comparing the results found for the capillary nematization of platelets and rods, we find remarkable differences. The most prominent one is the critical value of  $H$ . For platelets, we find  $H = 5.8D$ , for rods  $H = 2.67L$ . Thus, the critical capillary width for platelets is twice as large as that for rods, when measured in the natural length scale of the respective system. Similar behaviour is exhibited by the correlation length  $\xi$  that governs the decay both of the one-body density at large distances from a perturbation (such as a wall) and the pair correlation function at large separation of the particles. For platelets  $\xi_1/D = 0.66$  (at the isotropic side of the free IN interface) and  $\xi_N/D = 0.675$  (at the nematic side of the interface); for rods  $\xi_1/L = 0.335$  and  $\xi_N/L = 0.332$  [56]. Hence the correlation length of platelets (measured on the length scale of the particle) is about twice as large as that of rods.

Comparing the values for the shift in chemical potential at the capillary critical point with respect to the bulk value,  $\Delta\mu$ , we find  $\Delta\mu = 0.25k_B T$  for rods and  $\Delta\mu = 0.06k_B T$  for platelets. Recalling equation (13), we see that  $\Delta\mu$  is proportional to the IN interfacial tension  $\gamma_{IN}$  and inversely proportional to the IN density jump  $\rho_I - \rho_N$ . The interfacial tension  $\gamma_{IN} = 0.0266k_B T/D^2$  for platelets is much smaller than that for rods, which is  $\gamma_{IN} = 0.16k_B T/(Ld)$ . This significant difference is, however, partially compensated by a difference in the density jump, leading together to a smaller shift for platelets.

After completion of the current work we became aware of a very recent computer simulation study by Piñeiro *et al* [50]. These authors have investigated a system of hard cut spheres with aspect ratio (thickness over diameter) of 0.1 confined between either parallel plates or hard walls that act on the particle centres. Our current model of platelets is attained as the limit of cut spheres with vanishing aspect ratio. The results of the Gibbs ensemble computer simulations of [50] are reproduced in our figure 2(b). The shift of the simulation data to higher densities as compared to the DFT in bulk,  $L/H = 0$ , is due to the finite aspect ratio considered in the simulations. Apart from this effect a very similar shape of the binodal is found. Piñeiro *et al* quote a critical wall separation of  $4D$ , which is similar in magnitude to our value of  $5.8D$ .

## Acknowledgments

We thank M Dijkstra, R van Roij, H N W Lekkerkerker, D van der Beek, J Phillips, D Cheung and A J Masters for useful discussions. This work is supported by the EPSRC, HP Labs Bristol (Liquid Crystals Group), and by the SFB-TR6/D3 ‘Colloidal dispersions in external fields’ of the German Science Foundation (Deutsche Forschungsgemeinschaft).

## References

- [1] Zocher H 1925 *Z. Anorg. Chem.* **147** 91
- [2] Bawden F C, Pirie N W, Bernal J D and Fankuchen I 1936 *Nature* **138** 1051
- [3] Onsager L 1949 *Ann. (New York) Acad. Sci.* **51** 627
- [4] Vroege G J and Lekkerkerker H N W 1992 *Rep. Prog. Phys.* **55** 1241

- [5] Frenkel D and Eppenga R 1982 *Phys. Rev. Lett.* **49** 1089
- [6] Bates M and Frenkel D 1998 *Phys. Rev. E* **57** 4824
- [7] van der Kooij F M, Kassapidou K and Lekkerkerker H N W 1998 *J. Phys. Chem. B* **102** 7829
- [8] van der Kooij F M, Kassapidou K and Lekkerkerker H N W 2000 *Nature* **106** 868
- [9] van der Beek D, Petukhov A V, Oversteegen S M, Vroege G J and Lekkerkerker H N W 2005 *Eur. Phys. J. E* **16** 253
- [10] van der Beek D and Lekkerkerker H N W 2003 *Europhys. Lett.* **61** 702
- [11] van der Beek D and Lekkerkerker H N W 2004 *Langmuir* **20** 8582
- [12] Wijnhoven J E G J, van 't Zand D D, van der Beek D and Lekkerkerker H N W 2005 *Langmuir* **21** 10422
- [13] van der Beek D, Schilling T and Lekkerkerker H N W 2004 *J. Chem. Phys.* **121** 5423
- [14] van der Beek D, Petukhov A V, Davidson P, Ferre J, Jamet J P, Wensink H H, Vroege G J, Bras W and Lekkerkerker H N W 2006 *Phys. Rev. E* **73** 041402
- [15] Zhang Z X and van Duijneveldt J S 2006 *J. Chem. Phys.* **124** 154910
- [16] Pizzey C, van Duijneveldt J S and Klein S 2004 *Mol. Cryst. Liq. Cryst.* **409** 51
- [17] Zhang S D, Reynolds P A and van Duijneveldt J S 2002 *J. Chem. Phys.* **117** 9947
- [18] Zhang S D, Reynolds P A and van Duijneveldt J S 2002 *Mol. Phys.* **100** 3041
- [19] Wensink H H and Lekkerkerker H N W 2004 *Europhys. Lett.* **66** 125
- [20] Wensink H H, Vroege G J and Lekkerkerker H N W 2001 *J. Phys. Chem. B* **105** 10610
- [21] Harnau L, Costa D and Hansen J P 2001 *Europhys. Lett.* **53** 729
- [22] Oversteegen S M and Lekkerkerker H N W 2004 *J. Chem. Phys.* **120** 2470
- [23] Bier M, Harnau L and Dietrich S 2005 *J. Chem. Phys.* **123** 114906
- [24] Martinez-Raton Y and Cuesta J A 2002 *Phys. Rev. Lett.* **89** 185701
- [25] Rosenfeldt S, Karpuk E, Lehmann M, Meier H, Lindner P, Harnau L and Ballauff M 2006 *ChemPhysChem* **7** 2097
- [26] Dijkstra M and van Roij R 2005 *J. Phys.: Condens. Matter* **17** 3507
- [27] Poniewierski A 1993 *Phys. Rev. E* **47** 3396
- [28] van Roij R, Dijkstra M and Evans R 2000 *Europhys. Lett.* **49** 350
- [29] van Roij R, Dijkstra M and Evans R 2000 *J. Chem. Phys.* **117** 17
- [30] Dijkstra M, van Roij R and Evans R 2001 *Phys. Rev. E* **63** 051703
- [31] Dijkstra M 2004 *Phys. Rev. Lett.* **93** 108303
- [32] Roth R, van Roij R, Andrienko D, Mecke K R and Dietrich S 2002 *Phys. Rev. Lett.* **89** 088301
- [33] Harnau L and Dietrich S 2002 *Phys. Rev. E* **65** 021505
- [34] Harnau L, Rowan D and Hansen J-P 2002 *J. Chem. Phys.* **117** 11359
- [35] Harnau L and Dietrich S 2002 *Phys. Rev. E* **66** 051702
- [36] Bier M, Harnau L and Dietrich S 2004 *Phys. Rev. E* **69** 021506
- [37] Esztermann A, Reich H and Schmidt M 2006 *Phys. Rev. E* **73** 011409
- [38] Rosenfeld Y 1989 *Phys. Rev. Lett.* **63** 980
- [39] van der Beek D, Reich H, van der Schoot P, Dijkstra M, Schilling T, Vink R, Schmidt M, van Roij R and Lekkerkerker H N W 2006 *Phys. Rev. Lett.* **97** 087801
- [40] Reich H, Dijkstra M, van Roij R and Schmidt M 2007 *J. Phys. Chem. B* **111** 7825
- [41] Evans R and Marini Bettolo Marconi U 1987 *J. Chem. Phys.* **86** 7138
- [42] Evans R 1990 *J. Phys.: Condens. Matter* **2** 8989
- [43] Sheng P 1982 *Phys. Rev. A* **26** 1610
- [44] Telo da Gama M M and Tarazona P 1990 *Phys. Rev. A* **41** 1149
- [45] Mao Y, Bladon P, Lekkerkerker H N W and Cates M E 1997 *Mol. Phys.* **92** 151
- [46] Cheung D L and Schmid F 2004 *J. Chem. Phys.* **120** 19
- [47] Lagomarsino M, Dogterom M and Dijkstra M 2003 *J. Chem. Phys.* **119** 6
- [48] de las Heras D, Velasco E and Mederos L 2004 *J. Chem. Phys.* **120** 10
- [49] de las Heras D, Velasco E and Mederos L 2005 *Phys. Rev. Lett.* **94** 017801
- [50] Piñeiro M M, Galindo A and Parry A O 2007 *Soft Matter* **3** 768
- [51] Evans R 1992 *Fundamentals of Inhomogeneous Fluids* ed D Henderson (New York: Dekker) chapter 3, p 85
- [52] Ohnesorge R 1994 Dichtestruktur und Schmelzen von Kristallen und ihren Oberflächen *PhD Thesis* Ludwig-Maximilians-Universität München, München
- [53] Ohnesorge R, Löwen H and Wagner H 1993 *Europhys. Lett.* **22** 245
- [54] Ohnesorge R, Löwen H and Wagner H 1994 *Phys. Rev. E* **50** 4801
- [55] Telo da Gama M M, Tarazona P, Allen M P and Evans R 1990 *Mol. Phys.* **71** 801
- [56] Shundyak K 2004 Interfacial phenomena in hard rod fluids *PhD Thesis* Utrecht University, Utrecht